Formation, control, and dynamics of *N* localized structures in the Peyrard-Bishop model

Elías Zamora-Sillero,[1,*] A. V. Shapovalov,[2,3,†] and Francisco J. Esteban[4,‡]
[1]*Departamento de Fisica Aplicada I, E.U.P. Universidad de Sevilla Virgen de Africa 7, 41011 Sevilla, Spain*
[2]*Laboratory of Mathematical Physics, Tomsk Polytechnical University, 30th Lenin Avenue, 634050 Tomsk, Russia*
[3]*Department of Theoretical Physics, Tomsk State University, 36th Lenin Avenue, 634050 Tomsk, Russia*
[4]*Cell Biology Section, Department of Experimental Biology, University of Jaen, Jaen, Spain*
(Received 2 June 2007; published 6 December 2007)

We explore in detail the creation of stable localized structures in the form of localized energy distributions that arise from general initial conditions in the Peyrard-Bishop (PB) model. By means of a method based on the inverse scattering transform we study the solutions of PB model equations obtained in the form of planar waves whose amplitudes are described by the nonlinear Schrödinger equation (NLS). For localized initial conditions different from the pure *N*-soliton shape, we have obtained analytical results that predict and control the number, amplitude, and velocity of the NLS solitary waves. To verify the validity of these results we have carried out numerical simulations of the PB model with the use of realistic values of parameters and the initial conditions in the form of planar waves whose modulated amplitudes are given by the examples studied in the NLS. In the simulations we have found that *N* localized structures arise in agreement with the prediction of the analytical results obtained in the NLS.

DOI: 10.1103/PhysRevE.76.066603 PACS number(s): 05.45.Yv, 87.10.+e

I. INTRODUCTION

During the past decades the study of DNA has been an active and priority focus in research. Particularly, the nonlinear field of science pays special attention to the processes that take place at the base pair scale [1]. Many of the models, such as those proposed by Englander *et al.* [2] and by Peyrard and Bishop (PB) [3]; have achieved a remarkable success in qualitative and, sometimes, quantitative description of morphofunctional phenomena previously observed in DNA experimentally (see, e.g., [4]).

Most of the studies fulfilled in the framework of the above-mentioned applied theoretical models refer to the DNA melting and the formation of bubbles and localized structures. These bubbles play a vital role in DNA processes such as replication, recombination, and reparation, or in the DNA transcription to several types of RNA including those involved in the protein synthesis. Among the processes that have been described using bubbles and solitary waves one can find the following: the binding of specific enzymes to DNA (e.g., DNA polymerases, recombinases, helicases, or RNA polymerases) and the thermal evolution of enzyme-created bubbles [5]; the displacement of a bubble from the promoter to the coding regions [6–14]; the process of energy collection in the active regions under the enzyme action [15–20]; the openings of bubbles in the start sites of transcription [21–24].

The use of localized bubblelike structures in explaining these phenomena sets the problem of their creation and stability. In the past years it was found by many investigators that this is a rather complicated and substantial problem itself. In the framework of the PB model, Daumont and coworkers [25,26] have shown that the discreteness of the system causes the instability of the extended solutions. They tend to self-modulate evolving to localized solitonlike modes that interact nonelastically and grow the largest ones at the expense of the smallest [27]. It gives a possible path to the collecting of energy. Thermal fluctuations, which exist in the molecule due to the physiological temperature, are shown to be a pathway to energy localization and formation of localized structures [26,28–30]. On the other hand, it has recently been shown by Kalosakas *et al.* how a combination of these thermal fluctuations, sequence specificity, and nonlinearity induce large and slow bubbles in the chain that coincide with the localization of start sites of transcription [21–24]. Within the Englander model and with the use of random initial conditions, Cuenda and Sánchez [8] have obtained localized structures disposed in the transcription starting points employing the same sequence that Kalosakas *et al.* used. Finally, the curvature and twisting of molecular strands have been proposed to be responsible for a mechanism of bubble generation [31]. As one can see, the creation of localized structures in DNA models is a quite complicated problem in which the nonlinearity, discreteness, fluctuations, global dynamics of the molecule, heterogeneity of the sequence, and peculiarities of the initial conditions play an essential role.

In this work we aim to contribute a step in the above-described direction studying the creation process of solitonlike structures from localized initial conditions. In the Peyrard and Bishop model [3] and in the helicoidal model proposed by Barbi [32], using the multiple scale expansion (MSE) technique [33] and its generalization for vectorial systems [34], respectively, it is possible to obtain the analytical expression for approximate solutions in the form of modulated plane waves called breathers. The amplitude of these solutions is governed by the NLS equation. If the initial amplitude corresponds to the 1-soliton of NLS, planar wave with localized amplitude emerges. This solitary wave has been proposed as a possible precursor of the transcription process by means of trapping this breather in extended re-

*ezamora80@us.es
†shpv@phys.tsu.ru
‡festeban@ujaen.es

gions of DNA where the coupling constant is weaker [15]. Our objective is to show that these kinds of solutions do not appear only in cases when an appropriate pure soliton initial condition for the amplitude is introduced in the system. Given an initial condition in a form of a modulated wave, we use a powerful method based on the inverse scattering transform (IST) [35], that has been used successfully in solving different mathematical and physical problems [36–42], to study and control the conditions of formation, the number and properties of localized structures which can arise from an initial condition significantly different from the solitary wave discussed above. Subsequently, we introduce these initial conditions into the PB model with realistic values of parameters [43] and perform direct numerical simulations which demonstrates an excellent agreement between our numerical results and analytical predictions.

The paper structure is as follows. In Sec. II we introduce the general PB-like DNA model. In Sec. III we sketch the MSE technique that allows us to obtain the equation that governs the amplitude of planar waves in the form of NLS. In Sec. IV we present, using the inverse scattering transform formalism for NLS, general conditions of the existence of N solitonlike solutions. The latter means the existence of planar waves with localized modulated amplitude in the PB model. There we also give some examples of nonsoliton initial amplitudes, find out the conditions under which these amplitudes evolve towards N localized robust structures, and check these results by numerical simulations of NLS. In Sec. V, we study the dynamics of these solutions in the PB model with DNA parameters by means of direct numerical simulations, using the modulated planar waves, whose amplitudes are described in the examples discussed above, as initial conditions. We show the creation and evolution of solitary waves which are found to be in excellent agreement with analytical predictions and compare the time and space scales of these solutions with the typical ones in the biological processes under our study. Finally, Sec. VI summarizes our main results and implications.

II. PB MODEL

The difference between DNA and other biopolymers is the storage of genetic information that allows the cell machinery to build various types of RNAs and, on the next step, proteins. The DNA bases form the code that specifies the RNA properties and the protein composition. The process of reading the DNA code, called transcription [44], involves large amplitude nonlinear motions of the bases. This fact has focused the attention of physicists in the description, focused on the motion of the bases, of the molecule internal dynamics. The movement of the bases can be divided into torsional, longitudinal, and transversal displacements [6]. These movements are not independent of each other; however, the experimental results show that the time scale of the transversal movements is two or three times smaller than the others [45]. Thus, one can apply the adiabatic approximation [46] and separate the transversal dynamics from others.

The transversal dynamics can be studied by means of the PB model [3]. It is a one-dimensional model that describes the relative distance between each pair of complementary bases. In spite of the simplicity of the PB model, it can provide a good qualitative and quantitative description of the denaturalization of the molecule [4,43]. The Hamiltonian function of this model can be written as

$$H = \sum_n \frac{1}{2} m \left(\frac{dU_n}{dT} \right)^2 + \frac{1}{2} \tilde{K} (U_n - U_{n-1})^2 + \tilde{V}(U_n). \quad (1)$$

Here U_n denotes the relative distance between bases divided by $\sqrt{2}$, m is the base mass, $\tilde{K}$ is the rigidity of the harmonic potential of interaction between two bases of the same chain, and $\tilde{V}(U_n)$ is the potential of interaction between opposite bases representing the hydrogen bonds. For the PB model, $\tilde{V}(U_n)$ is chosen as follows $\tilde{V}(U_n) = D[\exp(-dU_n) - 1]^2$.

The evolution equations are

$$m \frac{d^2 U_n}{dT^2} = \tilde{K}(U_{n+1} + U_{n-1} - 2U_n) - \omega_0^2 \frac{dV}{dU_n}, \quad (2)$$

where $\tilde{V} = \omega_0 V$, and V is dimensionless. If we make the change of variables

$$u_n = bU_n, \quad t = \sqrt{\frac{\omega_0 b^2}{m}}, \quad K = \frac{\tilde{K}}{\omega_0 b^2}, \quad (3)$$

where $\omega_0 = D$ and $b = d$ for the PB model, the evolution equations become

$$\ddot{u}_n = K(u_{n+1} + u_{n-1} - 2u_n) - \frac{dV(u_n)}{du_n}. \quad (4)$$

They form a system of nonlinear ODEs which cannot be solved exactly. In spite of this fact, there are techniques [19,20,33,34,47,48] that allow us to construct approximate solutions of (4), find and study localized solutions.

III. SMALL AMPLITUDE MODULATED WAVES SOLUTIONS. NLS EQUATION

Following the ideas of Remoissenet [33], we will look for small solutions around the minimum of the potential $V(u_0)$. These solutions are of the form of a modulated amplitude carrier wave

$$u_n(t) = \epsilon \{F_1(t) e^{i\theta_n} + \epsilon [F_0(t) + F_2(t) e^{2i\theta_n}] + \text{c.c.}\}, \quad (5)$$

where $\theta_n = qna - \omega t$, a being the distance between bases. The frequency and the wave vector are related by

$$\omega^2 = (\omega_0')^2 + 4K \sin^2 \left(\frac{qa}{2} \right). \quad (6)$$

By substituting (5) in (4) we obtain

$$
\begin{aligned}
&(\ddot{F}_{1,n} - 2i\omega\dot{F}_{1,n} - \omega^2 F_{1,n})e^{i\theta_n} \\
&\quad + \epsilon\ddot{F}_{0,n} + \epsilon(\ddot{F}_{2,n} - 4i\omega\dot{F}_{2,n} - 4\omega^2 F_{2,n})e^{2i\theta_n} \\
&\quad = K(F_{1,n+1}e^{ika} + F_{1,n-1}e^{-ika} - 2F_{1,n})e^{i\theta_n} \\
&\qquad + \epsilon K(F_{0,n+1} + F_{0,n-1} - 2F_{0,n}) \\
&\qquad + \epsilon K(F_{2,n+1}e^{2ika} + F_{2,n-1}e^{-2ika} - 2F_{2,n})e^{2i\theta_n} - (\omega_0'^2) \\
&\qquad \times [F_{1,n}e^{i\theta_n} + \epsilon F_{0,n} + \epsilon F_{2,n}e^{2i\theta_n} \\
&\qquad + \epsilon\alpha(F_{1,n}^2 e^{2i\theta_n} + 2F_{1,n}F_{1,n}^*) \\
&\qquad + 2\epsilon^2\alpha(F_{1,n}F_{0,n} + F_{1,n}^* F_{2,n})e^{i\theta_n} + 3\epsilon^2\beta F_{1,n}^2 F_{1,n}^* e^{i\theta_n}],
\end{aligned}
\tag{7}
$$

where

$$
f = \left.\frac{\partial^2 V}{\partial u_n^2}\right|_{u_0}, \quad g = \left.\frac{1}{2}\frac{\partial^3 V}{\partial u_n^3}\right|_{u_0}, \quad h = \left.\frac{1}{3!}\frac{\partial^4 V}{\partial u_n^4}\right|_{u_0},
$$

$$
(\omega_0')^2 = f, \quad \alpha = \frac{g}{f}, \quad \beta = \frac{h}{f}. \tag{8}
$$

Now we suppose that $F_{j,n}$ varies slowly in space and time in comparison with the carrier wave. So, if we define

$$
X = \epsilon n a, \quad T = \epsilon t, \tag{9}
$$

we can write $F_j = F_j(X,T)$, that is called the semidiscrete approximation [33] in which the phase is treated exactly, and only the continuum approximation is used in the envelope function F_j. It was shown [25] that this approach can keep many specific features of the discrete systems. By substituting $F_j(X,T)$ in Eq. (7) and equating the terms of equal exponents we get

$$
\begin{aligned}
&\frac{\epsilon^2}{2\omega}F_{1TT} - 2i\omega F_{1T} - \epsilon^2\left[\frac{Ka^2\cos(qa)}{2\omega}\right]F_{1XX} \\
&\quad - i\epsilon\left[\frac{2aK\sin(qa)}{2\omega}\right]F_{1X} - \epsilon^2 Q'|F_1|^2 F_1 + O(\epsilon^3) = 0
\end{aligned}
$$

$$
F_0 = -2\alpha|F_1|^2 + O(\epsilon^2)
$$

$$
F_2 = \frac{\alpha F_1^2}{3 + \left[\frac{16K}{(\omega_0')^2}\right]\sin^4\left(\frac{qa}{2}\right)} + O(\epsilon^2), \tag{10}
$$

where

$$
Q = \frac{(\omega_0')^2}{2\omega}\left[4\alpha^2 - \frac{2\alpha^2}{3 + \left[\frac{16K}{(\omega_0')^2}\right]\sin^4\left(\frac{qa}{2}\right)} - 3\beta\right].
$$

To obtain (10) we have used the relation

$$
\begin{aligned}
&F_{j,n+1}e^{ijqa} + F_{j,n-1}e^{-ijqa} - 2F_{j,n} \\
&\quad \simeq \cos(jqa)a^2\frac{\partial^2 F_j}{\partial x^2} + 2ia\sin(jqa)\frac{\partial F_j}{\partial x} - 4\sin^2\left(\frac{jqa}{2}\right)F_j.
\end{aligned}
\tag{11}
$$

New variables

$$
Z = X - V_g T, \quad s = \epsilon T, \tag{12}
$$

transform (10) into the nonlinear Schrödinger equation

$$
iF_{1s} + PF_{1ZZ} + Q|F_1|^2 F_1 = 0, \tag{13}
$$

where

$$
V_g = \frac{d\omega}{dk} = \frac{Ka}{\omega}\sin(qa),
$$

$$
P = \frac{Ka^2}{2\omega}\left[\cos(qa) - \frac{K}{\omega^2}\sin^2(qa)\right]. \tag{14}
$$

Therefore, the evolution of the planar wave amplitude (5) is governed by the NLS equation. To study the localization of energy in the PB model (4), we should analyze the NLS equation and look for solutions, for which at least a part of the initial energy is stored in permanent localized structures. That is, we will look for modulated waves with localized amplitudes. This is the content of the next section.

IV. DESCRIPTION AND CONTROL OF N LOCALIZED STRUCTURES IN NLS

In the previous section we have seen how modulated waves obtained in the PB model can be described by the NLS (13). This equation is integrable by means of the IST method [35] and has N-soliton solutions when

$$
QP > 0. \tag{15}
$$

By changing the variables

$$
\tau = Qs, \quad y = \sqrt{\frac{Q}{2P}}Z, \tag{16}
$$

we can present the NLS in its standard form

$$
iF_{1\tau} + \frac{1}{2}F_{1yy} + |F_1|^2 F_1 = 0. \tag{17}
$$

In a class of functions that decrease at infinity the solution of Eq. (17) is a sum of localized and quite robust solitary waves and radiation [35]. Given the eigenvalue problem

$$
\begin{cases}
i\psi_y^{(1)} + F_1^*(y,0)\psi^{(2)} = \lambda\psi^{(1)}, \\
-i\psi_y^{(2)} + F_1(y,0)\psi^{(1)} = \lambda\psi^{(2)},
\end{cases}
\tag{18}
$$

the number of solitary waves is equal to the number of eigenvalues of the discrete spectrum, $\{\lambda_n = \zeta_n + i\eta_n, n = 1,\ldots N, \eta_n > 0\}$. Their velocity is proportional to the real part of the corresponding eigenvalue, $V_n = -2\zeta_n$, and their amplitude and width are related to the imaginary part, $A_n = -2\eta_n$. If the initial condition makes the reflection coef-

ficient of the eigenvalue problem (18) to be null, then the solution of (17) is formed only by solitons without any radiation [35]. It means that there are solutions of Eq. (13) in which the modulated amplitude $F_1(na,t)$ of Eq. (5) is localized. Then, all the models described by the Hamiltonian (1), that meet (15), can have solutions in the form of waves with a localized modulated amplitude. It allows localized concentrations of energy.

If we have only one eigenvalue in the discrete spectrum $\lambda=\zeta+i\eta$, the 1-soliton solution of (17) takes the form

$$F_1(y,\tau) = -2\eta \frac{e^{i[2\zeta y - 2(\zeta^2-\eta^2)(\tau-\tau_0)]}}{\cosh\{2\eta(y-y_0-2\zeta t)\}}. \tag{19}$$

After undoing the change of variables made in (9), (10), (12), (16), we substitute (19) in (5) and obtain the localized solution of the DNA model (4) that corresponds to the 1-soliton case [49]

$$\begin{aligned} u_n(t) = {} & 2\epsilon A \operatorname{sech}\left[\frac{\epsilon}{L_e}(na - V_e t)\right]\cos(\mathbb{Q}na - \Omega t) \\ & - 2\alpha\epsilon^2 A^2 \operatorname{sech}^2\left[\frac{\epsilon}{L_e}(na - V_e t)\right] \\ & \times\left(1 - \frac{1}{3 + \frac{16K}{(w_0')^2}\sin^4\left(\frac{qa}{2}\right)}\cos(2(\mathbb{Q}na - \Omega t))\right), \end{aligned} \tag{20}$$

where

$$v_e = 2\zeta\sqrt{2PQ}, \quad v_c = \sqrt{2PQ}\frac{\zeta^2-\eta^2}{\zeta},$$

$$A = \sqrt{\frac{v_e^2 - 2v_c v_e}{2PQ}}, \quad L_e = \frac{2P}{\sqrt{v_e - 2v_c v_e}},$$

$$V_e = V_g + \epsilon v_e, \quad \mathbb{Q} = q + \epsilon\frac{v_e}{2P}, \quad \Omega = \omega + \epsilon\left(\frac{v_e}{2P}\right)[V_g + \epsilon v_c]. \tag{21}$$

However, to be sure that the localization of energy is a robust result in the PB model, such localization should not appear only when the appropriate N-soliton solution is introduced as an initial condition in the NLS. From the IST point of view, it means that if $F_1(y,0)$ is not a reflectionless potential, the solutions $F_1(y,\tau)$ are not, strictly speaking, solitons because the radiation is present in the system. The next question arises: will permanent localized structures emerge in these cases or not. Rigorous results [50] show that all solutions can be decomposed into solitonlike solutions and radiation. In other words, given a nonsoliton initial condition, the system can group some of the energy in solitonlike structures while the rest of the energy is spread in the form of radiation. Then, after a transient time, we will again have a robust localization of energy in the system.

We are interested in such initial conditions, $F_1(y,0)$, that allow us to solve analytically the eigenvalue problem (18) and, therefore, classify and control the localized structures that emerge during the system evolution.

A. Square initial condition

Let us take the initial condition, $F_1(y,0)$, in the form

$$F_1(y,0) = \begin{cases} \rho e^{i\theta}, & y \in [c, c+g], \\ 0, & y \notin [c, c+g], \end{cases} \tag{22}$$

and substitute it in (18) which now can be written, for $y \in [c,c+g]$, in the following way

$$\left[\partial_{yy} - \frac{F_{1y}(y,0)}{F_1(y,0)}\partial_y + \lambda^2 + |F_1(y,0)|^2 + i\lambda\frac{F_{1y}(y,0)}{F_1(y,0)}\right]\psi^{(2)} = 0,$$

$$\psi^{(1)} = -\frac{1}{F_1(y,0)}(\lambda\psi^{(2)} + i\psi_y^{(2)}). \tag{23}$$

The solution of (23) is

$$\psi = N_{II}\begin{pmatrix} -\frac{1}{F_1(y,0)}(\lambda + \partial_y), \\ 1 \end{pmatrix} A e^{iy\sqrt{\Omega}} + B e^{-iy\sqrt{\Omega}}, \tag{24}$$

where $\Omega=\rho^2+\lambda^2$. For $y<c$ and $y>c+g$ we obtain

$$\psi = N_I\begin{pmatrix} 1 \\ 0 \end{pmatrix} e^{-i\lambda y}, \quad y < c,$$

$$\psi = N_{III}\begin{pmatrix} 0 \\ 1 \end{pmatrix} e^{i\lambda y}, \quad y > c+g. \tag{25}$$

Imposing the continuity in $y=c$ and $y=c+g$, we find the following quantization condition for the eigenvalues:

$$\frac{\lambda + \sqrt{\Omega}}{\lambda - \sqrt{\Omega}} e^{-2ig\sqrt{\Omega}} = 1. \tag{26}$$

To satisfy this equation, it is necessary that

$$\xi_n = i\eta_n, \quad \zeta_n = 0, \quad \eta_n > 0. \tag{27}$$

Then the eigenvalues are pure imaginary numbers and are given by the roots of the transcendental equation

$$\beta_n - S\cos(\beta_n) = \pi\left(\frac{1}{2} - n\right), \tag{28}$$

where

$$\sqrt{\rho^2 - \eta_n^2} = \rho\cos(\beta_n), \quad \eta_n = \rho\sin(\beta_n),$$

$$S = \int_{-\infty}^{+\infty} dy |F_1(y,0)|. \tag{29}$$

The number of eigenvalues can be obtained from (28)

$$N = \operatorname{ent}\left[\frac{S}{\pi} + \frac{1}{2}\right]. \tag{30}$$

It is interesting to mention that S must be greater than its threshold value $S_0=\pi/2$ to obtain localized solutions. For the

values smaller than S_0, all the initial energy will be spread in the form of radiation without any localization of energy [57]. On the other hand, the pure imaginary eigenvalues guarantee that the centroid of energy of the system is of null velocity and different N localized structures are not separated from each other.

B. Exponential initial condition

Let the function $F_1(y,0)$ be chosen as

$$F_1(y,0) = \begin{cases} \rho e^{\vartheta y}, & y \le y_0, \\ 0, & y > y_0, \end{cases} \tag{31}$$

where $\vartheta = a + ib$.

For $y \le y_0$, we substitute it in (23) and change the variable $z = \frac{\rho}{a} e^{ay}$ and $\psi^{(2)} = z^{\mu}\varphi(z)$, where $\mu = \frac{a+ib}{2a}$. Then Eq. (23) becomes

$$z^2\varphi_{zz} + z\varphi_z + \left[z^2 - \left(\mu - i\frac{\lambda}{a} \right)^2 \right] \varphi = 0, \tag{32}$$

with the boundary condition

$$\lim_{z \to 0} \varphi = 0. \tag{33}$$

The solution of (32) is the Bessel function

$$\varphi(z) = J_{\nu}(z), \quad \nu = \mu - i\frac{\lambda}{a}. \tag{34}$$

So for $y \le y_0$ we have

$$\psi = N_I \begin{pmatrix} -\dfrac{a}{F_1(y,0)} \left(iz\partial_z + \dfrac{\lambda}{a} \right) \\ 1 \end{pmatrix} z^{\mu} J_{\nu}(z).$$

For $y > y_0$, the eigenvalue problem (18) is trivial and gives

$$\psi = N_{II} \begin{pmatrix} 0 \\ 1 \end{pmatrix} z^{i\frac{\lambda}{a}}.$$

If we require the solution to be continuous at $y = y_0$, the following equation

$$\nu J_{\nu}(z_0) + z_0 J'_{\nu}(z_0) = 0,$$

must be valid, where

$$z_0 = S = \int_{-\infty}^{+\infty} dy |F_1(y,0)| = \frac{\rho}{a} e^{ay_0}. \tag{35}$$

Taking into account that the following recurrence relation

$$J_{\nu-1}(z) = \frac{\nu}{z} J_{\nu}(z) + J'_{\nu}(z),$$

is always fulfilled for the Bessel functions, we obtain the quantization condition

$$J_{\nu-1}(z_0) = 0. \tag{36}$$

For a given z_0, it has the solutions ν_n $n = 1, 2, 3, \ldots$. Therefore, the discreet spectrum is the set

$$\left\{ \nu_n - 1 = -\frac{1}{2} + \frac{\eta_n}{a} + i\left(\frac{b}{2a} - \frac{\zeta_n}{a} \right),\ J_{\nu_n - 1}(z_0) = 0 \right\}. \tag{37}$$

The indices ν_n of the Bessel functions $J_{\nu_n}(z_0)$ are real because z_0 is real [51]. In our case it leads to $\nu_n > 1/2$ and $\zeta_n = \frac{b}{2}$ for all n. Therefore, all the eigenvalues have equal real parts and then all the localized structures generated from the initial conditions have equal velocities. Finally, the number of the solitary waves and their amplitudes can be determined by the roots of the equation

$$j_{\nu_n, s} - \nu_n - (3s - 1) = z_0 - \nu_n - (3s - 1), \tag{38}$$

where $j_{\nu_n, s}$ is the sth-zero of J_{ν_n}.

In this case we again have a threshold value $S_0 \simeq \pi$ to create localized structures. It is interesting to point out that for $\pi/2 < S < \pi$ the energy is spread without localization. On the contrary, for these values of S a one solitonlike structure emerges in case of the square initial condition.

C. Numerical simulations for NLS

All the results and predictions shown in Secs. IV A and IV B involve the hypothesis that the radiation has a negligible effect on the process of formation of solitonlike structures and on their dynamics. Therefore, it is necessary to perform numerical simulations of the NLS (17) to check the analytical results obtained above. These simulations have been carried out by means of a standard fourth-order Runge-Kutta scheme with free boundary conditions. In all the simulations the relative change of the charge and energy is less than 10^{-4} and 10^{-3}, respectively [58]

In our simulations we have used different initial conditions and compared the numerical results with the analytical predictions discussed in previous sections. The conclusion of our numerical simulation program is that the analytical results are completely valid even when a significant amount of radiation is present in the system. In addition we show that if the initial conditions are slightly changed in order to make them smoother, the overall picture of the emergence of localized structures is completely similar to that obtained in the original cases. It means that our analytical results are suitable to predict localization properties in the PB model (4). In case of square initial conditions (22) we show the existence of a threshold value of S to create solitonlike solutions. For $S = 0.3 < \pi/2$ [see Figs. 1(a) and 1(b)] we can observe that the initial condition decays into radiation without the formation of any localized structure, whereas for $S > \pi/2$ we have found the creation of stable localized structures [see Figs. 1(c) and 1(d) for $S = 7.7$, $(N = 2)$ and Figs. 1(e) and 1(f) for $S = 14$, $(N = 4)$]. In both cases the number of localized structures agrees well with the prediction of analytical formula (30). It is interesting to mention that the velocity of the localized structures is zero in all cases, as the solution of the eigenvalue problem shows (27). So, the structures do not separate from each other giving rise to a complex dynamics [see, i.e., Figs. 1(c) and 1(e)].

For the exponential initial condition (31) we check the close relation between the number and properties of localized structures and the value of S. Again we have a threshold

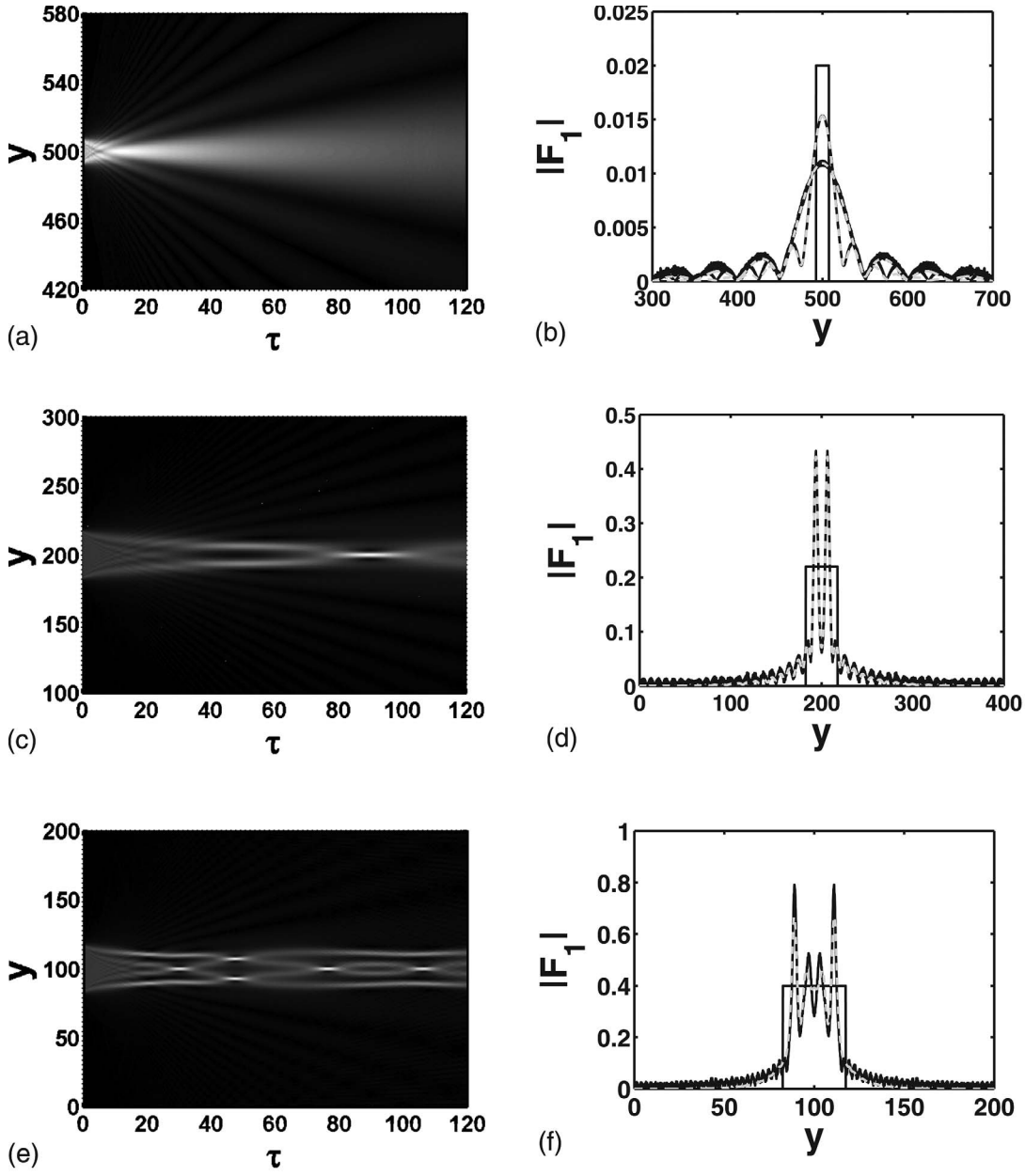

FIG. 1. The complete dynamics of the solution of the NLS (17), $|F_1(y,\tau)|$, in the case of square initial conditions (22) is presented in the left panels. In panel (a): $\rho=0.02$, $g=15$, $\theta=\pi/4$, and $S=0.3$ ($N=0$). In panel (c): $\rho=0.22$, $g=35$, $\theta=\pi/4$, and $S=7.7$ ($N=2$). In panel (e): $\rho=0.4$, $g=35$, $\theta=\pi/4$, and $S=14$ ($N=4$). In all cases black color corresponds to $|F_1|=0$, and white to $|F_1|=0.025$, 0.7, and 2.0 for the panels (a), (c), and (e), respectively. $|F_1(y,\tau)|$ is presented in the right panels for square (22) (black curves) and squarelike (39) (gray dashed curves) initial conditions. In panel (b): $\tau=0$, 70, and 120. In panel (d): $\tau=0$ and 49.75. In panel (f): $\tau=0$ and 14. In all cases the parameters used are the same as in their correspondent left panel with $h=1$ for squarelike initial conditions (39).

value. For $S=0.4531<\pi$ the initial condition decays into radiation without the creation of any permanent localized structure [see Figs. 2(b) and 3(a)]. It can be determined graphically [see Fig. 2(a)] that Eq. (38) has no root, therefore the analytical results predict that a solitonlike structure will not be formed, which is in total agreement with the simulation evidence. For $S>\pi$ solitonlike structures emerge. The number of them is equal to the number of roots of (38). Namely, one soliton for $S=3.3986$ [see Figs. 2(c), 2(d), and 3(b)] and three solitons for $S=10.53$ [see Figs. 2(e), 2(f), and 3(c)]. We have measured the velocity of the localized structures and obtained $V=0.78\pm0.01$ in the case of $N=1$ [see Fig. 2(d)] and $V_1=0.7993\pm0.0007$, $V_2=0.793\pm0.002$, $V_3=0.7793\pm0.0015$ for $N=3$ [see Fig. 2(f)]. The velocity predicted by the analytical results is $V_n=0.7854$ in all the cases. We see that for all the solitonlike structures the difference between the analytical and numerical velocities is smaller than 2 percent.Therefore, it is correct, in first approximation, to neglect the contribution of the radiation to the dynamics and formation of the solitonlike structures.

We have found that the numerical data agree well with the analytical results in the cases of the square and exponential

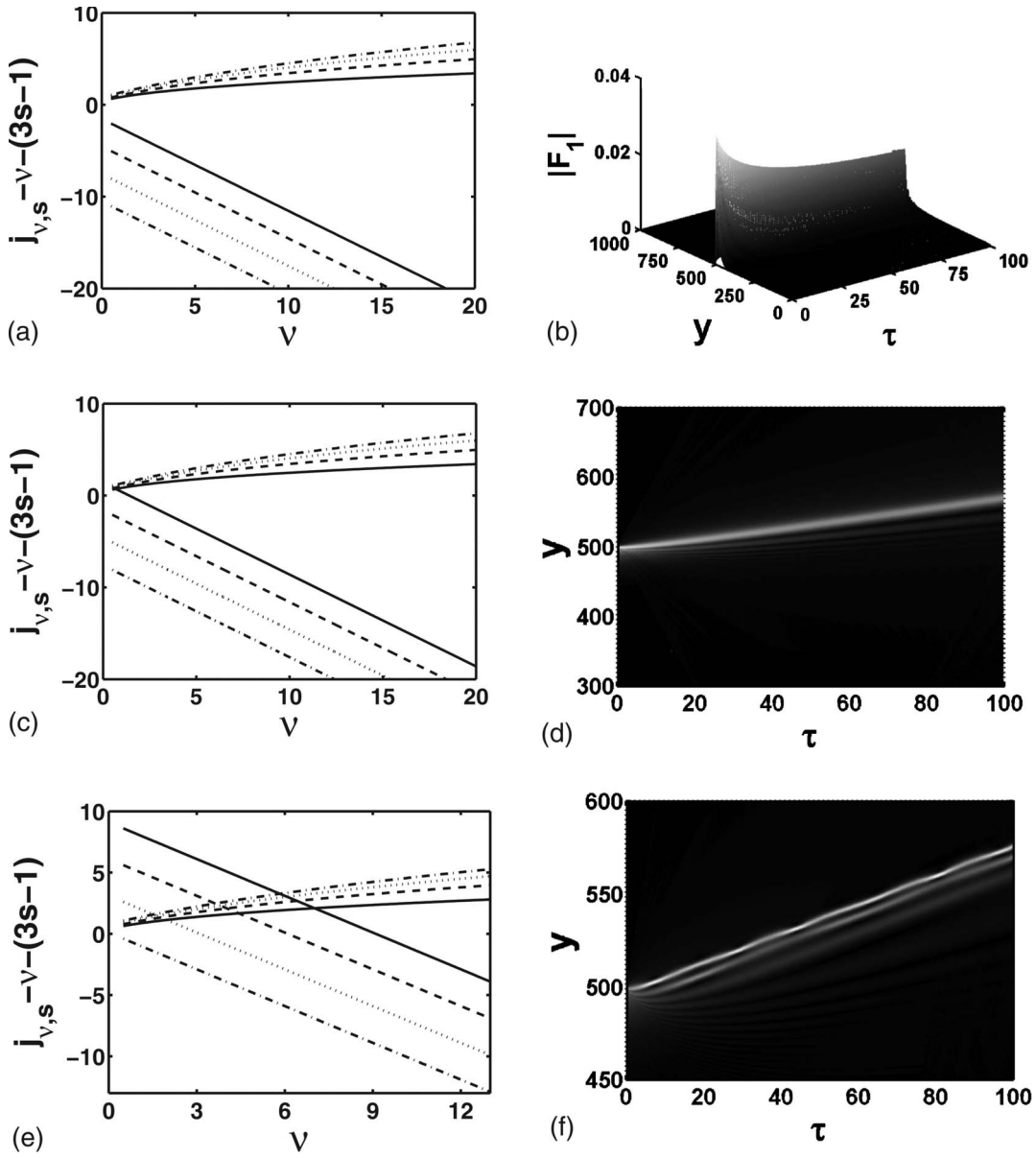

FIG. 2. The left panels show the graphical solution of Eq. (38). One may see the intersection of the functions $j_{\nu_n,s}-\nu_n-(3s-1)$ and $z_0-\nu_n-(3s-1)$ for $s=1$ (solid line), $s=2$ (dashed line), $s=3$ (point line), and $s=4$ (point-dashed line). Panel (a): $S=z_0=0.4531$, there is no root. For panel (c), $S=z_0=3.3986$, there is one root for $s=1$. For panel (e), $S=z_0=10.53$, there are three roots for $s=1$, $s=2$, and $s=3$. The right panels present the complete dynamics of the solution of the NLS (17), $|F_1(y,\tau)|$, for exponential initial conditions (31). Panel (b): $b=\pi/4$, $\rho=2\times10^{-17}$, $a=0.07$, and $S=0.4531$ ($N=0$). Panel (d): $b=\pi/4$, $\rho=1.5\times10^{-16}$, $a=0.07$, and $S=3.3986$ ($N=1$). Panel (f): $b=\pi/4$, $\rho=4.65\times10^{-16}$, $a=0.07$, and $S=10.53$ ($N=3$). In all these cases black corresponds to $|F_1|=0$, and white to $|F_1|=0.035$, 0.25, and 1.2 for the panels (b), (d), and (f), respectively.

initial conditions. However, in the theory presented in previous sections, the function $F_1(y,0)$ must be smooth because we look for a slowly varying amplitude in space and time. We propose new initial conditions similar to the square one (22)

$$F_1(y,0)=\frac{\rho}{2}\left\{\tanh\left(\frac{y-c}{h}\right)-\tanh\left(\frac{y-(c+g)}{h}\right)\right\}e^{i\theta}, \tag{39}$$

and to the exponential one (31)

$$F_1(y,0)=\begin{cases}\rho e^{\vartheta y}, & y\le p_0,\\ \rho_0 e^{-\sigma^2(y-p_0)^2+iby}, & y>p_0,\end{cases} \tag{40}$$

where

$$p_0=y_0-\frac{1}{a}\ln\left(\frac{a\sqrt{\pi}}{2\sigma}+1\right),\quad \rho_0=\rho e^{ap_0},$$

to check whether the overall dynamics of the system remains unchanged if the initial conditions are smoother.

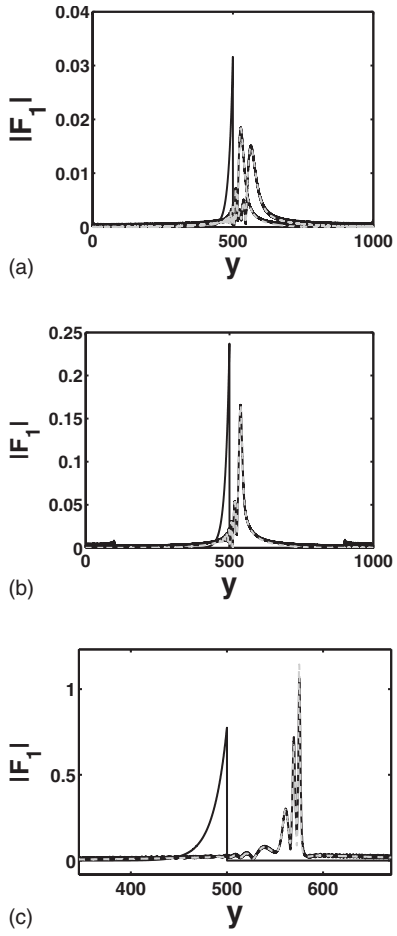

FIG. 3. The panels present $|F_1(y,\tau)|$ for exponential (31) (black curves) and exponential-like (40) (gray dashed curves) initial conditions. Panel (a) corresponds to the parameters $b=\pi/4$, $\rho=2\times10^{-17}$, $a=0.07$, $S=0.4531$, and $\sigma=1$ $(N=0)$ for $\tau=0$, 49.8, and 100. Panel (b) corresponds to the parameters $b=\pi/4$, $\rho=1.5\times10^{-16}$, $a=0.07$, $S=3.3986$, and $\sigma=1$ $(N=1)$ for $\tau=0$ and 60. Panel (c) corresponds to the parameters $b=\pi/4$, $\rho=4.65\times10^{-16}$, $a=0.07$, $S=10.53$, $\sigma=1$, $(N=3)$ for $\tau=0$ and 100.

Given the parameters $\{\rho,c,g,\theta,a,b,y_0\}$, the new initial conditions (39) and (40) have the same value of S as the original ones. In case of the square and exponential-like initial conditions (39), (40), we have performed numerical simulations with $\sigma=h=1$ and the same parameters used in previous ones. If we compare the solutions, for all the cases, with the solutions obtained when (22) and (31) are used as initial conditions, we find them to be qualitatively identical. We obtain the same number of solitary structures and the same patters of evolution [see Figs. 1(b), 1(d), and 1(f) in case of the square], and [Figs. 3(a)–3(c) for the case of the exponential]. Thus, we can conclude that it is reasonable to use the results obtained in previous sections to study the localization of energy in the PB model due to the negligible effect of the radiation and the robustness of the creation of localized structures when the initial conditions are slightly changed.

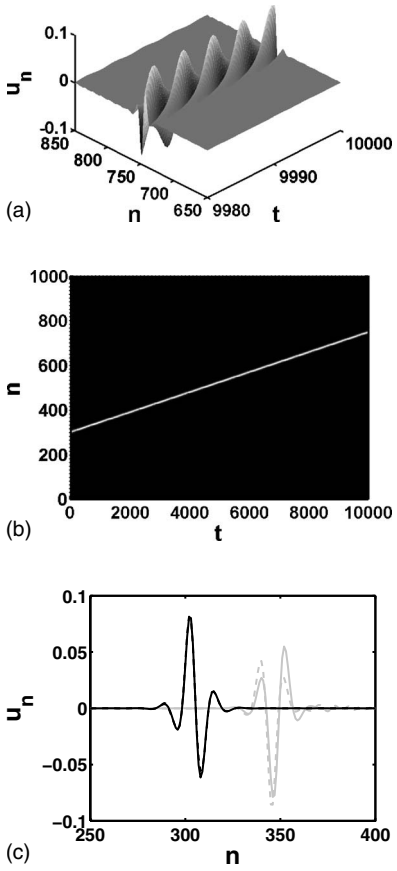

FIG. 4. The three panels show direct numerical simulations of the PB model where the initial condition (20) is used, which corresponds to the pure 1 soliton. Panels (a) and (b) present the dynamics of $u_n(t)$ and $E_n(t)$ for $v_e=3$, $v_c=1$, $q=0.01$ Å^{-1}, and $\epsilon=0.05$, respectively. For this set of parameters $\tau_p=87.20$. In panel (b) black corresponds to $E_n=0$ and white to $E_n=9\times10^{-3}$. Panel (c), using the same parameters as in the previous panels, presents u_n versus n at the time instant $t=100$, of the order of τ_p [the solid black curve corresponds to the analytical solution (20), and the dashed black curve to the numerical simulation; both curves can not be distinguished by the eyes], and in $t=1000$, much greater than τ_p (the solid gray curve corresponds to the analytical solution (20), and the gray dashed curve to the numerical simulation).

V. DIRECT NUMERICAL SIMULATIONS IN THE PB MODEL

To study the creation and stability of localized structures in the PB model, it is not enough to formulate the problem in terms of the NLS (17) that governs the dynamics of the amplitude of modulated waves (5). The transformation from the equation of motion of the bases (4) to the NLS involves some approximations. So, the results obtained in the framework of the NLS must be compared with direct numerical simulations in the PB model with realistic values of parameters.

In all simulations we use a fourth-order Runge-Kutta scheme. We choose absorbing boundary conditions to avoid an artificial large amount of radiation that can affect the creation process and the dynamics of the localized structures. Under these boundary conditions the total energy is not con-

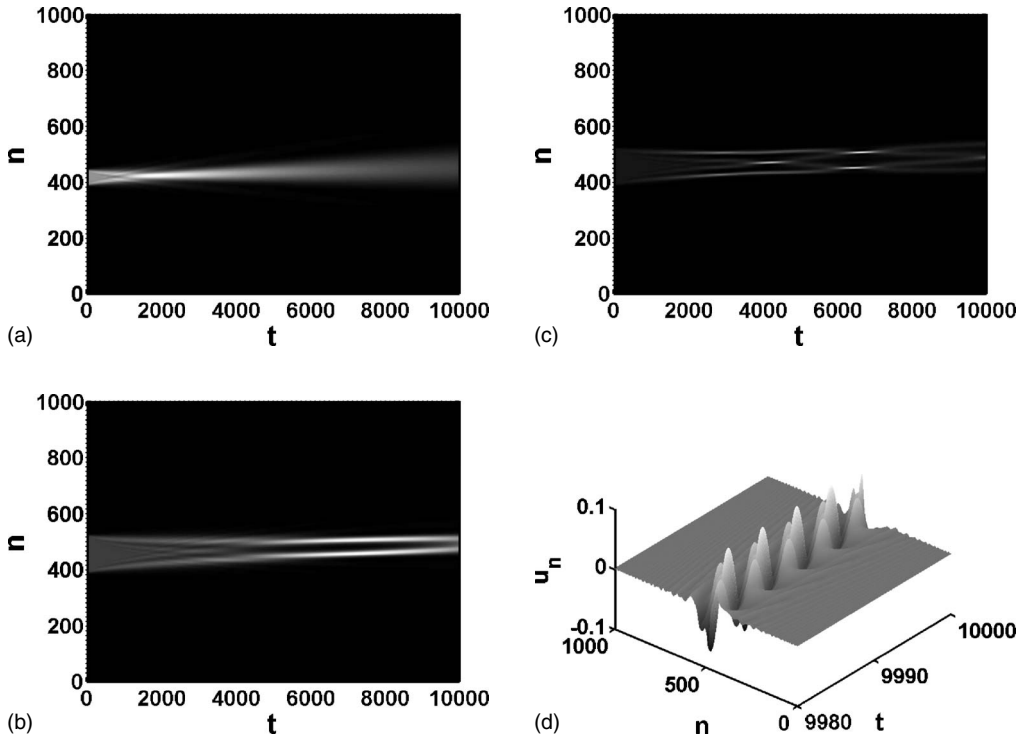

FIG. 5. The panels show direct numerical simulations of the PB model. For all the panels the square-like function (39) was used as initial condition for the amplitude of the planar waves (5) after the changes of variables (9), (12), and (16). In panels (a), (b), and (c) the dynamics of $E_n(t)$ is represented. In panel (a): $c=100$, $g=15$, $h=1$, $\rho=0.02$, $\theta=\pi/4$, $q=0.01$ Å^{-1}, $\epsilon=0.05$, and $S=0.3$ ($N=0$). In panel (b): $c=100$, $g=35$, $h=1$, $\rho=0.22$, $\theta=\pi/4$, $q=0.01$ Å^{-1}, $\epsilon=0.05$, and $S=7.7$ ($N=2$). In panel (c): $c=100$, $g=35$, $h=1$, $\rho=0.4$, $\theta=\pi/4$, $q=0.01$ Å^{-1}, $\epsilon=0.05$, and $S=14$ ($N=4$). In all these cases black corresponds to $E=0$, and white to $E=6.5\times10^{-6}$, 1.7×10^{-3}, and 1.7×10^{-2} for the panels (a), (b), and (c), respectively. Panel (d) presents the dynamics of $u_n(t)$ for the same parameters used in (c).

served in the system, but in all the simulations, the relative change of the energy is less than 10^{-6} before the radiation reaches the boundaries of the system.

It has been shown [25] that the dynamics in the PB model depends drastically on the choice of the parameter values used in the model. We choose realistic parameters for a chain of guanine-cytosine, $a=3.4$ Å, $D=0.35$ eV, $d=4.45$ Å^{-1}, $\tilde{K}=0.104$ eV/Å^2, $m=300$ a.m.u. [43], leading to $K=0.15$. In our simulations we use initial conditions in the form of a modulated planar wave (5) with a wave vector q and frequency ω related by the dispersion equation (11). The initial amplitude form, F_n, corresponds to the 1-soliton (20), squarelike (39), and exponential-like (40) shape after the changes of variables (9), (12), and (16). We vary the parameters of these functions in order to change the value of S and compare the localization of energy in the DNA model with the analytical results obtained in previous sections for the evolution of the initial amplitude in the framework of the NLS. After numerical simulations we conclude that the number and properties of the emerged solitonlike structures agree well with the predictions of our analytical calculations. Even in cases where no localized solutions are formed, the energy spreading is so slow that these structures have physical entity due to their long lifetime. Therefore a strong localization of energy in the system is possible when we do not have an initial amplitude that corresponds to a pure N-soliton case. It implies that in the PB model the localization of energy from localized initial conditions is a very robust phenomena.

When the initial condition (20), which corresponds to the exact 1-soliton solution of NLS (19), is used, we can observe that the energy is well localized and travels with constant velocity [see Figs. 4(a) and 4(b)]. It can be seen that for a time period of the order of the propagation time scale of the solution, $\tau_p=(\epsilon V_e/L_e)^{-1}$, the agreement between the numerical simulation and the analytical formula is very accurate [see solid and dashed black lines in Fig. 4(c)], in spite of the approximations that we have performed to obtain the analytical formula (19). For times much greater than the propagation time scale, small tails start to appear in the solution obtained by means of the numerical simulation due to the nonintegrability of the PB model. This makes the difference between the analytical and numerical solutions larger [see solid and dashed gray lines in Fig. 4(c)].

The solution that corresponds to the exact 1-soliton has been widely studied in the context of the PB model [15]. Our aim is to show that energy localization can arise from different initial conditions. This means that the system responds to many different initial states in a similar way and, therefore, the localization of energy is a robust process in the PB model. In the cases of the square and exponential-like initial conditions, we have chosen exactly the same parameters that were used in the previous section. This allows us to directly compare the results obtained in the frameworks of the DNA model and the NLS. For both square (39) and exponential-like initial conditions (40) we observe again that if $S<S_0$, the initial energy spreads without the formation of permanent localized structures [see Figs. 5(a) and 6(a)]. Whereas for S

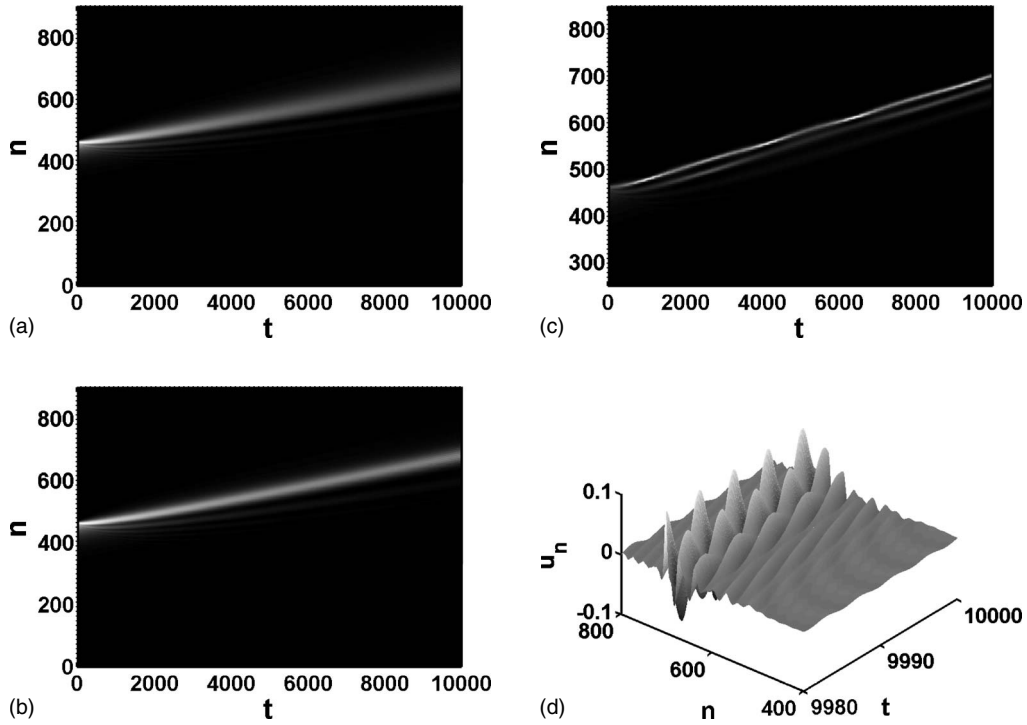

FIG. 6. The panels show direct numerical simulations of the PB model. For the right panels the exponential-like function (40) was used as the initial condition for the amplitude of the planar waves (5) after the changes of variables (9), (12), and (16). In panel (a), (b), and (c) the dynamics of $E_n(t)$ is presented. Panel (a): $a=0.07$, $b=\pi/4$, $\rho=2\times10^{-17}$, $S=0.4531$, $(N=0)$, $\sigma=1$, $q=0.01$ Å^{-1}, and $\epsilon=0.05$. Panel (b): $a=0.07$, $b=\pi/4$, $\rho=1.5\times10^{-16}$, $S=3.3986$, $(N=1)$, $\sigma=1$, $q=0.01$ Å^{-1}, and $\epsilon=0.05$. Panel (c) for $a=0.07$, $b=\pi/4$, $\rho=4.65\times10^{-16}$, $S=10.53$, $(N=3)$, $\sigma=1$, $q=0.01$ Å^{-1}, and $\epsilon=0.05$. In all these cases black corresponds to $E=0$, and white to $E=1\times10^{-5}$, 5.5×10^{-4}, and 1.7×10^{-3} for the panels (a), (b), and (c), respectively. Panel (d) presents the dynamics of $u_n(t)$ for the same parameters used in (c).

$>S_0$ the localized structures are formed and stabilized in a perfect agreement with the predictions of the analytical results [see Figs. 5(b), 5(c), 6(b), and 6(c)]. In these figures it can also be observed that the patterns of evolution of the energy in the PB model are very similar to those which were obtained in case of the NLS equation. This fact shows the validity of the semidiscrete approximation. So, it can be seen that localized stable solutions arise from different localized initial conditions.

To give a quantitative description of the energy localization in our simulations, we measure the magnitude

$$L(t)=\sum_n E_n, \quad \langle n\rangle-\sqrt{\langle\Delta n^2(0)\rangle}\le n\le\langle n\rangle+\sqrt{\langle\Delta n^2(0)\rangle}, \tag{41}$$

where

$$\langle n\rangle=\frac{\sum_{n=1}^{N} nE_n}{\sum_{n=1}^{N} E_n}, \quad \langle\Delta n^2\rangle=\frac{\sum_{n=1}^{N}(n-\langle n\rangle)^2E_n}{\sum_{n=1}^{N} E_n}, \tag{42}$$

E_n being the energy that corresponds to the system (4).

The function $L(t)$ informs us about the energy that is localized at an interval around the centroid of energy of the system. The length of this interval is related to the width of the initial distribution of energy. When the initial conditions meet $S>S_0$, the evolution of $L(t)$ [see Figs. 7(a) and 7(b)] shows that after $t=10000$, $(2.11\times10^{-11}$ s), a large amount of energy is concentrated in a region compared in size with the interval of the initial localization, as we expected. In all the cases this amount of energy is greater than 80 percent of the energy that was initially in this interval. It must be pointed out that the localization of energy during a time period of 2.11×10^{-11} s, which is much greater than the typical time scale of the transversal movements in DNA (10^{-14} s), allows to provide physical sense to these localized structures in spite of the localization of energy showing a time dependence that may lead to a delocalization at later times. When $S<S_0$, no permanent localized structures are created but the energy loss is very slow [see black dashed lines in Figs. 7(a) and 7(b)]. After $t=10000$, $(2.11\times10^{-11}$ s), more than 40 percent of the energy is still concentrated near the centroid of energy. Therefore, even if the localizations of energy are not permanent, they have physical meaning due to their long lifetimes in comparison with the time scale of the transversal movements of the bases. The cases of the exponential-like initial conditions for which $\Delta n(0)=27.68$ (b.p.) [see Figs. 6(a)–6(c)] are of special relevance. The length $\Delta n(0)$ is very similar to the size of the transcription bubble [52–54] This fact implies that the energy can remain localized for a very large period of time if it is deposited in a region of the length of the transcription bubble.

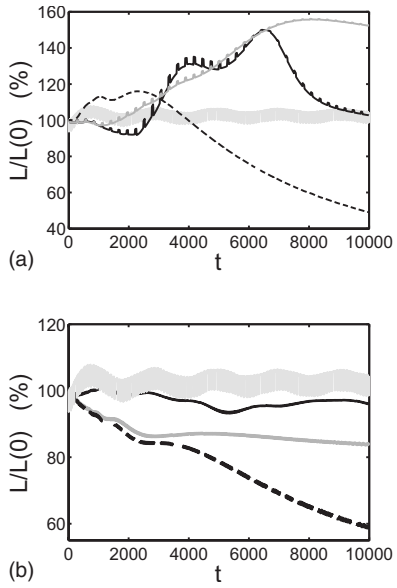

FIG. 7. Evolution of the function $L(t)/L(0)$. In panel (a) the solid light gray curve corresponds to the solution related with the pure 1-soliton case (20). The others correspond to the case of squarelike initial conditions (39) after the changes of variables (9), (12), and (16). The dashed black curve corresponds to the case of $S=0.3$ ($N=0$), the solid dark gray curve to $S=7.7(N=2)$, and the solid black curve to $S=14(N=4)$. In panel (b) the solid light gray curve corresponds to the solution related with the pure 1-soliton case (20). The others correspond to the case of exponential-like initial conditions (39) after the changes of variables (9), (12), and (16). The dashed black curve corresponds to the case of $S=0.4531$ ($N=0$), the solid dark gray curve to $S=3.3986$ ($N=1$), and the solid black curve to $S=10.53$ ($N=3$).

We can conclude that not only the localized solutions that arise from a pure *N*-soliton initial conditions are possible in the PB model. It is shown that localized structures, whose numbers and properties are controlled by the parameter *S*, can be created from different initial conditions in a good agreement with the analytical and numerical results obtained for the NLS. Moreover, the characteristic time of energy spreading is much greater than the time scale of the transversal movements of the bases even in case of initial conditions with $S<S_0$ from which we do not expect localized structures.

VI. CONCLUSIONS

In the framework of the PB model we have explored the process of localization of energy from different initial localized distributions of energy. We have proposed a solution in the form of modulated planar waves (5). Also, using the so-called semidiscrete approximation [33], we have shown that the NLS governs the evolution of the amplitude of these waves (17). In previous works [1,15,32–34] the amplitude described by means of the 1-soliton solution was substituted in the planar waves solution. The dynamics of this structure was studied paying special attention to its properties of localization. In the present paper we analyze, by means of a method based on the IST [35], the NLS that governs the amplitude. Using initial conditions different from pure *N*-soliton solutions, we have obtained analytical results which describe and control the number, amplitude, and velocity of the solitonlike structures that emerge from the initial conditions. Among these results, we must emphasize the existence of control parameter *S*, which is related to the area of the modulus of the initial amplitude, that rules the existence of solitonlike structures. For each kind of initial condition, a threshold value S_0 exists. If $S<S_0$, all the energy is spread without the formation of permanent structures. These analytical results have been checked through numerical simulation of the NLS obtaining a very good agreement between them, even when the initial conditions were slightly changed and there was a large amount of radiation in the system.

The study of the NLS is not enough to analyze the localization of energy in the PB model. The approximations carried out to obtain the equation of evolution of the amplitude oblige to check the results obtained in the framework of the NLS by means of direct numerical simulations of the PB model (4) with realistic values of the parameters. From the initial conditions in the form of planar waves with the amplitudes given by the functions studied in the NLS, we have observed that localized structures were created and their number and properties were controlled by the parameter *S* in full agreement with the analytical and numerical results obtained for the NLS. In case of initial conditions with $S>S_0$, more than 80 percent of the energy has been found to remain concentrated in a region comparable with the initial localization after a time much longer than the typical time scale of the transversal movement of the bases in DNA. When $S<S_0$, permanent localized structures do not emerge. However, the rhythm of energy loss is so slow that the localization of energy has physical meaning due to its long lifetime in comparison with the time scale of the transversal movements of the bases. So, we can conclude that in the PB model with realistic DNA parameters, *N* permanent localized structures can arise from initial conditions that are not related to the *N*-soliton solution of the NLS. Even in case of initial states, for which localized structures do not appear, the time scale of the energy spreading is much greater than the typical scales of movement in the transversal dynamics. Therefore, the localization of energy in the PB model, in absence of thermal fluctuations, is quite a robust process where no specific initial conditions are required to achieve it.

It is important to point out that applications of these results in biology must be done with prudence. From a theoretical point of view, it is known that the stability and lifetime of localized solutions are very sensitive to such properties of the thermal fluctuations as viscosity and temperature [55,56].The DNA is in contact with a thermal bath in the cell. Therefore, the friction and thermal forces play an important role in its internal dynamics. So, it is necessary to explore the role of the thermal noise in the process of formation of localized structures to study the creation and dynamics of *N* localized structures in the PB model in a cell environment. On the other hand, such basic complex DNA functional processes as replication and transcription are controlled by means of the actions of proteins [44]. Therefore, to understand the DNA functioning, it is not enough to take into

account only the internal interactions. It is necessary to study the interplay between the internal motion (e.g., internal oscillations) in the DNA and the proteins involved in the processes.

ACKNOWLEDGMENTS

We would like to thank N. R. Quintero, A. Sánchez, L. V. Tsybulcko and V. Kilin for useful and interesting discussions on this work. This work was supported by the Ministerio de Ciencia y Tecnología of Spain under Grant No. FIS2005-973 (E.Z.S.), from the Junta de Andalucía through Projects No. FQM-0207 and No. 00481 (E.Z.S.), and from President of the Russian Federation Grant No. SS-5103.2006.2 (A.V.S). In addition, E.Z.S. acknowledges the hospitality of the Department of Mathematical Physics and the Laboratory of Mathematical Physics of Tomsk Polytechnic University. A.V.S. acknowledges the hospitality of the Department of Mathematical Analysis and Applied Physics I of the University of Sevilla.

[1] M. Peyrard, Nonlinearity **17**, 1 (2004).
[2] S. W. Englander, N. R. Hippel, A. J. Heeger, J. A. Krumhansl, and A. Litwin, Proc. Natl. Acad. Sci. U.S.A. **77**, 7222 (1988).
[3] M. Peyrard and A. R. Bishop, Phys. Rev. Lett. **62**, 2755 (1989).
[4] A. Campa and A. Giansanti, Phys. Rev. E **58**, 3585 (1998).
[5] D. Henning, J. R. F. Archilla, and J. M. Romero, J. R. Soc., Interface **2**, 89 (2005).
[6] L. V. Yakushevich, *Nonlinear Physics of DNA* (Wiley, Chichester, 2004).
[7] A. Campa, Phys. Rev. E **63**, 021901 (2001).
[8] S. Cuenda and A. Sánchez, Fluct. Noise Lett. **4**, 491 (2004).
[9] S. Cuenda and A. Sánchez, Phys. Rev. E **70**, 051903 (2004).
[10] S. Cuenda, A. Sánchez, and N. R. Quintero, Physica D **223**, 214 (2006).
[11] M. Salerno, Phys. Rev. A **44**, 5292 (1991).
[12] M. Salerno, Phys. Lett. A **167**, 49 (1992).
[13] M. Salerno and Yu. S. Kivshar, Phys. Lett. A **193**, 263 (1994).
[14] E. Lennholm and M. Hornquist, Physica D **177**, 233 (2003).
[15] Julian J-.L. Ting, and M. Peyrard, Phys. Rev. E **53**, 1011 (1996).
[16] K. Forinash, M Peyrard, and B. Malomed, Phys. Rev. E **49**, 3400 (1994).
[17] K. Forinash, T. Cretegny, and M. Peyrard, Phys. Rev. E **55**, 4740 (1997).
[18] J. Cuevas, F. Palmero, J. R. Archilla, and F. R. Romero, J. Phys. A **35**, 10519 (2002).
[19] T. Dauxois, M. Peyrard, and C. R. Willis, Physica D **57**, 267 (1992).
[20] T. Dauxois, M. Peyrard, and C. R. Willis, Phys. Rev. E **48**, 4768 (1993).
[21] G. Kalosakas, K. Ø. Rasmussen, A. R. Bishop, C. H. Cnoi, and A. Usheva, Europhys. Lett. **68**, 127 (2004).
[22] C. H. Cnoi, G. Kalosakas, K. Ø. Rasmussen, M. Hiromura, A. R. Bishop, and A. Usheva, Nucleic Acids Res. **32**, 1584 (2004).
[23] Z. Rapti, A. Smerzi, K. Ø. Rassmussen, A. R. Bishop, C. H. Choi, and A. Usheva, Phys. Rev. E **73**, 051902 (2006).
[24] S. Ares and G. Kalosakas, Nano Lett. **7**, 307 (2007).
[25] I. Daumont, T. Dauxois, and M. Peyrard, Nonlinearity **10**, 617 (1997).
[26] M. Peyrard, Physica D **119**, 184 (1998).
[27] O. Bang and M. Peyrard, Phys. Rev. E **53**, 4143 (1996).
[28] G. P. Tsironis, A. R. Bishop, A. V. Savin, and A. V. Zolotaryuk, Phys. Rev. E **60**, 6610 (1999).
[29] V. Muto, A. C. Scott, and P. L. Christiansen, Phys. Lett. A **136**, 33 (1989).
[30] V. Muto, A. C. Scott, and P. L. Christiansen, Physica D **44**, 75 (1990).
[31] P. V. Larsen, P. L. Christiansen, O. Bang, J. F. R. Archilla, and Yu. B. Gaididei, Phys. Rev. E **70**, 036609 (2004).
[32] M. Barbi, S. Cocco, and M. Peyrard, Phys. Lett. A **253**, 358 (1999).
[33] M. Remoissenet, Phys. Rev. B **33**, 2386 (1986).
[34] S. Cocco, M. Barbi, and M. Peyrard, Phys. Lett. A **253**, 161 (1999).
[35] V. E. Zaharov and A. B. Shabat, Zh. Eksp. Teor. Fiz. **61**, 118 (1971).
[36] L. S. Brizhik and A. S. Davydov, Phys. Status Solidi B **115**, 615 (1983).
[37] L. S. Brizhik, Yu. B. Gaididei, and A. A. Vakhnenko, Phys. Status Solidi B **146**, 650 (1988).
[38] L. S. Brizhik, Phys. Rev. B **48**, 3142 (1993).
[39] V. A. Donchenko, M. V. Kabanov, E. V. Lugin, A. A. Nalivaiko, and A. V. Shapovalov, Atmos. Oceanic Opt. **1**, 67 (1988) (in Russian).
[40] V. G. Bagrov, D. M. Gitman, M. C. Baldiotti, and A. D. Levin, Ann. Phys. **14**, 764 (2006).
[41] E. Zamora Sillero and A. V. Shapovalov, Phys. Rev. E **76**, 046612 (2007).
[42] Y. S. Kivshar and B. A. Malomed, Rev. Mod. Phys. **61**, 763 (1989).
[43] T. Dauxois, M. Peyrard, and A. R. Bishop, Phys. Rev. E **47**, 684 (1993).
[44] C. R. Calladine and H. R. Drew, *Understanding DNA* (Academic, London, 2002).
[45] J. A. McCammon and S. C. Harvey, *Dynamics of Proteins and Nucleic Acids* (Cambridge University Press, Cambridge, 1987).
[46] L. V. Yakushevich, J. Biosci. **26**, 305 (2001).
[47] S. Flach and C. R. Willis, *Nonlinear Excitations in Biomolecules*, edited by M. Peyrard (Springer-Verlag, Berlin, 1994).
[48] S. Flach and C. R. Willis, Phys. Rep. **295**, 181 (1998).
[49] M. Barbi, Ph.D. thesis, Tesi do Doctoratto, 1998 (unpublished).
[50] V. E. Zakharov, S. V. Manakov, S. P. Novikov, and L. P. Pitaevsky, *Theory of Solitons: The Inverse Scattering Method* (Plenum, New York, 1984).
[51] E. Janke, F. Emde, and F. Losch, *Tafeln Honerer Funktionen* (B. G. Teuber Verlagsgesellschaft, Stuttgart, 1960).

[52] B. F. Kahl, H. Li, and M. R. Paule, J. Mol. Biol. **299**, 75 (2000).
[53] A. L. Gnatt, P. Cramer, J. Fu, D. A. Bushnell, and R. D. Kornberg, Science **292**, 1876 (2001).
[54] D. Wang, D. A. Bushnell, K. D. Westover, C. D. Kaplan, and R. D. Kornberg, Cell **127**, 941 (2006).
[55] M. Gleiser and R. M. Haas, Phys. Rev. D **54**, 1626 (1996).
[56] R. M. Haas, Phys. Rev. D **57**, 7422 (1998).
[57] For a general initial condition $F_1(y,0)$, a soliton solution is possible if at least one point in the discrete spectrum exists among all the eigenvalue problem solutions (18). It can be shown [35] that it implies the neccesary condition $S>\ln(2+\sqrt{3})\simeq 1.32$. We can see in our examples that the threshold value S_0 is greater than 1.32 and depends on the concrete initial condition.
[58] It is well known that the NLS equation has an infinite number of conserved quantities [35] including the charge, $Q=\int_{-\infty}^{+\infty}dy|F_1|^2$ and the energy, $E=\int_{-\infty}^{+\infty}dy|F_{1,y}|^2-\int_{-\infty}^{+\infty}dy|F_1|^4$.